Liquid chromatography-electrospray ionization-tandem mass spectrometry method for quantitative estimation of new imiqualine leads with potent anticancer activities in rat and mouse plasma. Application to a pharmacokinetic study in mice

Adrien Chouchou, Bénédicte Marion, Christine Enjalbal, Céline Roques, Pierre Cuq, Pierre-Antoine Bonnet, Françoise M.M. Bressolle-Gomeni, Carine Deleuze-Masquéfa

Liquid chromatography-electrospray ionization-tandem mass spectrometry method for quantitative estimation of new imiqualine leads with potent anticancer activities in rat and mouse plasma. Application to a pharmacokinetic study in mice.

Adrien Chouchou[a], Bénédicte Marion[a], Christine Enjalbal[a], Céline Roques[a], Pierre Cuq[a], Pierre-Antoine Bonnet[a], Françoise M.M. Bressolle-Gomeni[b,*], Carine Deleuze-Masquéfa[a]

[a]*IBMM, Université de Montpellier, CNRS, ENSCM, Montpellier, France*

[b]*R&D Department, Pharmacometrica France, Longcol, La Fouillade, France*

*Corresponding author.

E-mail address: fbressolle@yahoo.fr (F.M.M. Bressolle-Gomeni).

Abstract

Imidazoquinoxaline derivatives (imiqualines) are a new series of anticancer compounds. Two lead compounds (EAPB0203 and EAPB0503) with remarkable in vitro and in vivo activity on melanoma and T-cell lymphomas have been previously identified. The modulation of the chemical structure of the most active compound, EAPB0503, has led to the synthesis of two compounds, EAPB02302 and EAPB02303, 7 and 40 times more active than EAPB0503 against A375 human melanoma cancer cell line, respectively. The aim of this study was to develop and validate a sensitive and accurate liquid chromatography-electrospray ionization-tandem mass spectrometry method to simultaneously quantify EAPB02303 and its potential active metabolite, EAPB02302, in rat and mouse plasma. Analytes were detected in multiple reaction monitoring acquisition mode using an electrospray ionization detector in positive ion mode. Following a liquid-liquid extraction with ethyl acetate, analytes and internal standard were separated by HPLC reversed-phase on a C18 RP18 Nucleoshell column (2.7 µm, 4.6 × 100 mm). The method was validated according to FDA and EMA Bioanalytical Method Validation guidelines. Standard curves were generated via unweighted quadratic regression of calibrators (EAPB02303: 1.95-1000 ng/mL, EAPB02302: 7.81-1000 ng/mL in rat plasma; EAPB02303: 0.98-1000 ng/mL, EAPB02302: 1.95-1000 ng/mL in mouse plasma). From the analysis of QC samples, intra- and inter-assay precision and accuracy studies demonstrated %R.S.Ds. < 12.5% and percent deviation from nominal concentration < 7%. Matrix effects (mean matrix factors from 91.8-108.5% in rat plasma; and from 90.4-102.4% in mouse plasma) and stability assays (recoveries > 90%) studies were acceptable and in accordance with the guidelines. No quantifiable carryover effect was observed. The LLOQs were 1.95 ng/mL for EAPB02303 and 7.81 ng/mL for EAPB02302 in rat plasma, and 0.98 ng/mL and 1.95 ng/mL for the two compounds in mouse plasma, respectively. This method was successfully implemented to support a mouse pharmacokinetic study following a single intraperitoneal administration of

EAPB02303 in male C57Bl/6 mice. The obtained pharmacokinetic parameters of EAPB02303 would be useful to optimize the dosing and the rhythm of administration for subsequent preclinical in vivo activity studies.

Keywords:

Imiqualines

Anticancer agent

EAPB02303 EAPB02302

LC/MRM-MS

Rat mouse plasma

Pharmacokinetics

1. Introduction

According to estimates from the International Agency for Research on Cancer (IARC), the cutaneous malignant melanoma incidence has presented an exponential increase around the world for over 7 decades [1,2]. Melanoma is an aggressive and heterogeneous skin cancer with a multifactorial development. The pathophysiological process implies a malignant transformation of the melanocytes under the influence of risk factors such as ultra-violet light exposure, genetic predisposition or also skin phenotype [3,4]. Despite the development of new anticancer agents by pharmaceutical industry [5], the mortality rate remains high and the cure rate low. Therefore, the development of compounds with original mechanisms of action is necessary.

Heterocyclic systems containing the quinoxaline moiety exhibit important biological activities. Many imidazoquinoxaline derivatives have shown interesting potential as active pharmaceutical products [6,7]. Our group is particularly involved in the study and development of new imidazo[1,2-*a*]quinoxaline compounds, also called imiqualines, which have been protected by different patents since 2008 [8] and granted in the USA on February 2013 and Canada on May 2016 [9,10].

Two active compounds, EAPB0203 and EAPB0503, have previously emerged as promising drugs with interesting antitumoral activities against a panel of human cancer cell lines including melanoma, T-lymphoma, myeloid leukemia and colon carcinoma [11-18]. EAPB0203 has shown significant in vitro cytotoxic activity against A375 human melanoma cell line, 110 and 45 times higher than fotemustine and imiquimod, respectively [11,15]. Tested in vivo in M4Be xenograft female Swiss Nude mice, EAPB0203 caused a significant decrease in tumor growth compared to vehicle control and fotemustine treatments [11,15]. EAPB0503 is 7-9 times more active than EAPB0203 on A375 human melanoma cell line and has been identified as our first lead compound [13]. Recently, EAPB0503 and its structural imidazo[1,2-*a*]quinoxaline

derivatives have demonstrated major microtubule-interfering agents properties [19]. Studies to determine the absorption, distribution, metabolism, excretion, and toxicology properties of EAPB0203 and EAPB0503 have also been investigated [14-18,20,21].

The modulation of the chemical structures of the first identified lead compound (nature and/or position of the substituents) affects and modifies its biological properties. Among the synthesized compounds, EAPB02303 and its *N*-demethylated derivative, EAPB02302, (Fig. 1) have recently been identified as new lead compounds due to their in vitro activities [22].

In order to perform in vivo studies, a method for assaying these compounds in biological matrices should be developed and validated. Furthermore, pharmacokinetic data are required to optimize doses and rhythm of administration during preclinical activity studies.

In previous papers, we have found that, in all species, the main metabolite of EAPB0203 and EAPB0503 is formed after *N*-demethylation [14,15,18]. So, in the present paper, a liquid chromatography-electrospray ionization-tandem mass spectrometry method (LC-ESI-MS/MS) was developed and validated to simultaneous quantify EAPB02303 and its potential active metabolite, EAPB02302, in rat and mouse plasma. The choice of these two types of matrix is justified by the fact that during the preclinical development of drugs, rat is one of the principal species to be studied and mice xenografts are the most used in vivo melanoma models. Then, the validated method was used during a pharmacokinetic study performed in mice after intraperitoneal administration of EAPB02303.

2. Materials and methods

2.1. Chemicals and reagents

EAPB02303 (4-(4-(methylamino)imidazo[1,2-*a*]quinoxalin-1-yl)benzene-1,2-diol; molecular weight, 306 Da), EAPB02302 (4-(4-aminoimidazo[1,2-*a*]quinoxalin-1-yl)benzene-1,2-diol; molecular weight, 292 Da) and the internal standard (IS) EAPB0602 (3-(4-

aminoimidazo[1,2-*a*]quinoxalin-1-yl)phenol; molecular weight, 276 Da) (Fig. 1), were synthesized by the "Oncopharmacochemistry and Cutaneous Pharmacotoxicology" laboratory (IBMM, Montpellier University, France). Briefly, they were synthesized in good yields via a bimolecular condensation of 2-imidazole carboxylic acid, followed by a coupling with ortho-fluoroaniline and subsequent substitution on the imidazole ring by Suzuki Cross-Coupling reaction using microwave assistance [22]. The purity of the compounds (higher than 99%) was evaluated by elementary analysis and NMR. They were stored at 20 °C protected from light.

Acetonitrile and ethyl acetate (HPLC grade) were obtained from Sigma-Aldrich (Saint-Louis, Missouri, USA). Dimethyl sulfoxide (DMSO), 3-[4,5-dimethylthiazol-2-yl]-2,5-diphenyltetrazolium bromide (MTT), isopropyl alcohol, and hydrochloric acid were obtained from Merck (Darmstadt, Germany). Ammonium formate and formic acid were purchased from VWR Chemicals (Radnor, Pennsylvania, USA). All chemicals were of the highest purity available.

Six different batches of drug free rat (from healthy male Sprague Dawley rats weighting 230-280g) and mouse (from Swiss mice weighting 20-25g) plasma pools were obtained from Janvier Labs (Le Genest Saint Isle, France). These plasma pools were obtained from blood collected on lithium heparinate to prevent coagulation. Blank matrices were aliquoted and stored at -80 °C until used. The same lot was used during the study in the preparation of standards and quality control (QC) samples. The other lots were used to verify the specificity of the method and the absence of matrix effect. Formate buffer pH 3 was prepared by dissolving 126 mg of ammonium formate in 1 L of purified water; the pH was adjusted with formic acid. Purified water was generated by a Milli-Q reagent water system (Millipore, Bedford, MA, USA).

2.2. In vitro cytotoxic activity study

A375 cell line was obtained from American Type Culture Collection (Rockville, Md., USA). Cells were maintained in Gibco™ Dulbecco's Modified Eagle Medium (DMEM, ThermoFisher Scientific, Illkirch-Graffenstaden, France) supplemented with 10% heat-inactived (56 °C) foetal bovine serum (FBS) (Polylabo, Paris, France), 2 mM L-glutamine, 100 IU/mL penicillin G sodium, 100 µg/mL streptomycin sulfate, and 0.25 µg/mL amphotericin B. Cells were cultured in a humidified atmosphere with 5% CO_2 at 37 °C. All studies were done with cells at 70 to 80% confluence. The day of experiment, cells were harvested with 0.02% trypsin, 0.05% ethylenediaminetetraacetic acid (EDTA, ThermoFisher Scientific) for 5 minutes at 37 °C, counted and resuspended. Then, 100 µL of cell suspension (i.e., 5000 cells/well) were seeded with a multichannel pipet into the individual wells of a 96-well tissue culture plate with lid (TPP, Trasadingen, Switzerland), and allowed to attach overnight. After 24 h of incubation, the medium was aspirated carefully from the plates using a sterile Pasteur pipette, and cells were exposed (in six replicates) (i) to vehicle controls (1% DMSO/culture medium and culture medium alone), (ii) vemurafenib at concentrations of 3.10^{-7} to 10^{-9} M, diluted in the culture medium, and (iii) EAPB02303 and EAPB02302 (3.10^{-7} to 10^{-9} M) dissolved in a mixture 1% DMSO/culture medium (v/v). Vemurafenib was chosen as reference instead of dacarbazine, fotemustine or imiquimod because this compound has shown improved rates of overall and progression-free survival in patients with previously untreated melanoma with the BRAF V600E mutation [23]. After 96 h of incubation, the supernatant of each well was aspirated and the cell viability was determined by MTT assay. The proliferation test is based on the color reaction of mitochondrial dehydrogenase in living cells by MTT. Thus, MTT (final concentration 5 mg/mL in phosphate-buffered saline pH 7.4 from ThermoFisher Scientific) was added to each well, which was then incubated at 37 °C in 5% CO_2 for 4 h. Thereafter, the supernatant was carefully aspirated and the colored crystals of produced formazan were

dissolved in 100 µL of a mixture of isopropyl alcohol and 1 M hydrochloric acid (96/4, v/v). The absorbance was measured at 570 nm on Microplate Reader (Dynatech MR 5000, France).

Cell proliferation was calculated as the ratio of absorbance of treated group divided by the absorbance of control group, multiplied by 100 to give a percentage proliferation. The individual cell line growth curves confirmed that all cell lines in control medium remained in the log phase of cell growth 96 h after plating. The IC_{50} values defined as the concentrations of drugs which produced 50% cell growth inhibition (i.e., 50% reduction of absorbance) were estimated from the sigmoidal dose-response curves.

2.3. Fragmentation pathways of EAPB02303 and EAPB02302

Mass spectra were acquired on a Synapt G2-S (Waters Milford, CA) equipped with a ESI source fitted with a lock spray for high resolution mass measurements and a QTof mass analyzer configuration. Nitrogen constituted both nebulizing and desolvation gas. MS and MS/MS data were recorded in the positive mode between *m/z* 50 and 500 Th with a scan time of 0.1 s and an interscan delay of 0.015 s. The source tuning consisted of a capillary voltage of 3 kV, a cone voltage of 30 V, a desolvation gas flow of 1000 L/h and source and desolvation temperatures of 140 °C and 450 °C, respectively. The mass spectrometer was calibrated using 1% phosphoric acid in H_2O/CH_3CN solution (50:50, v/v). Reference solutions of EAPB02303 and EAPB02302 dissolved in acetonitrile–purified water (50:50, v/v) were infused into the ESI source at a flow rate of 5 µL/min. Exact mass spectra measurements were performed across the entire mass range (*m/z* 50-500) upon high resolution acquisition mode (HRMS) using leucine enkephalin infused as the calibration standard via the lock spray system. In MS/MS experiments, the protonated molecular ion was selected as precursor ion on the first quadrupole, the second quadrupole analyzer was set in the rf mode using argon as collision gas, and the collision energy

varied from 25 to 50 eV to give optimal fragmentation. MassLynx v. 4.1 (Waters) software was used for data acquisition and processing.

2.4. Quantification of EAPB02303 and EAPB02302 in rat and mice plasma

2.4.1. LC-ESI-MS/MS analyses

Assay development and sample analysis were performed on an Agilent 1100 LC system (Agilent Technologies, Les Ulis, France) linked with an API 3000 tandem triple quadrupole mass spectrometer (ABSciex, Courtaboeuf, France). The chromatographic separation was conducted by injecting 5 µL of each reconstituted sample extract on a C18 RP18 Nucleoshell column (2.7 µm, 4.6 × 100 mm) from Macherey-Nagel (Düren, Germany) at 30 °C. A guard column (Nucleoshell RP 18, 2.7 µm, 4 × 2 mm) was used to safeguard the analytical column. A mixture of acetonitrile (eluent A) and 2 mM ammonium formate buffer pH 3 (eluent B) (70/30, v/v) was used as mobile phase at a flow rate of 0.5 mL/min without split. All solvents were filtered through a 0.20 µm millipore filter (Molsheim, France) before use and degassed 15 min in an ultrasonic bath. The autosampler was set at 4 °C.

Analytes were ionized in positive ion mode using ESI probe set at 400 °C. The curtain, nebulizer, and collision gases were nitrogen and were set at 8, 8 and 4 psi, respectively. The ion spray voltage was set at 5000 V, and the entrance potential at 10 V. Detection of EAPB02303 and EAPB02302 was performed using multiple reaction monitoring (MRM). The optimal MRM transitions for precursor ion $[M+H]^+$ to specific product ion were *m/z* 307 → 292 and *m/z* 307 → 278 for EAPB02303 (Fig1A-a of the online Data Supplement), *m/z* 293 → 104, *m/z* 293 → 90 and *m/z* 293 → 77 for EAPB02302 (Fig1B-a of the online Data Supplement), and *m/z* 277 → 117 for the internal standard. MRM transitions and optimal compound dependent parameters are given in Table 1. The acquisition dwell time was 150 ms for all transitions. Mass

spectra were collected in scan mode (*m/z* 50-500). The LC-MS/MS system was controlled and the analytical data were collected and processed using Analyst software version 1.5 (AB Sciex).

2.4.2. Stock and working solutions

Stock solutions of EAPB02303, EAPB02302 and internal standard (IS) were prepared individually in DMSO at 1 mg/mL. Two sets of stock solutions were prepared, one for the preparation of calibration standards and the other for the preparation of QC samples. They were stored at –20 °C until use.

Stock solutions were extemporaneously and serially diluted in the mobile phase as appropriate to yield working solutions ranging from 19.5 to 20000 ng/mL for EAPB02303, from 39.1 to 20000 ng/mL for EAPB02302 and at 2500 ng/mL for the internal standard. Unextracted solutions containing 3.91, 62.5 and 500 ng/mL of the two analytes and 125 ng/mL of IS in the mobile phase were injected before each run to check the performance of the LC-ESI−MS/MS system.

2.4.3. Preparation of calibration curves and QC samples

Drug-free plasma (200 µL from rat or 100 µL from mouse) was spiked with appropriate working solutions of EAPB02303 and EAPB02302. The final concentrations of plasma calibration standards were 1.95, 7.81, 15.6, 31.3, 62.5, 125, 250, 500 and 1000 ng/mL for EAPB02303, and 7.81 15.6, 31.3, 62.5, 125, 250, 500 and 1000 ng/mL for EAPB02302. In mouse plasma, the lowest calibration standard was at 0.98 ng/mL for EAPB02303 and 1.95 ng/mL for EAPB02302 (Tables 1 and 2 of the online Data Supplement). Different calibration curves were performed on the same day (n = 6) and on separate days (n = 14) in rat plasma. For mouse plasma, calibration curves were obtained on separate days (n = 6). Calibration curves were generated by plotting the peak area ratios (analyte/IS) versus the nominal concentrations.

Different models were tested: i) unweighted or weighted least-squares linear regression analysis ($Y = aX + b$) and ii) quadratic relationship ($Y = aX^2 + bX + c$) with Y = peak area ratio and X = nominal concentration. The regression curve was not forced through zero. The resulting equation parameters were used to calculate back-calculated concentrations for the calibrators that were statistically evaluated.

QC samples were prepared in the same way by spiking drug-free matrices with working solutions to provide low, medium, and high concentrations: 3.91, 46.9, 187 and 750 ng/mL for EAPB02303 and 11.7, 46.9, 187 and 750 ng/mL for EAPB02302. In mice plasma, additional QC samples were prepared at 1.95 ng/mL for EAPB02303 and 3.91 ng/mL for EAPB02302. QC samples were used during the study to determine matrix effect, extraction efficiencies and stability assays, as well as to evaluate accuracy and precision of the method.

2.4.4. Sample preparation

Calibration standards, QC samples, and study samples were processed using liquid-liquid extraction. The optimized sample pretreatment was as follows: to 200 µL of rat plasma or 100 µL of mouse plasma, 10 µL of the internal standard solution (2500 ng/mL) and 10 µL of 1% (v/v) formic acid in water were added. After vortex mixing for 15 s, 600 µL of ethyl acetate were added. The mixture was vigorously vortexed twice for 15 s and then centrifuged at 4 °C (5 min at 25,830*g*). The upper organic phase was removed and evaporated to dryness at 40 °C under a gentle stream of nitrogen. The residue was reconstituted in 200 µL of mobile phase. The mixture was vortexed for 15 s and then centrifuged at 4 °C (5 min at 9400*g*). One hundred microliters of the supernatant were transferred into polypropylene autosampler vials and a 5 µL volume was injected into the LC-MS/MS system.

2.4.5. Method validation

Method validation was performed based on the "guidance for Industry Bioanalytical Method Validation" recommended by the Food and Drug Administration (FDA) and the European Medicines Agency (EMA) [24-27].

The assay selectivity was investigated by using six individual lots of blank plasma. Each blank sample was extracted and chromatographed to determine the extent to which endogenous plasma components may contribute to chromatographic interference with EAPB02303 and EAPB02302. One hemolyzed plasma was also checked for specificity.

Intra-day accuracy and precision were determined by analyzing six replicates of each QC sample on the same day against a calibration curve. Inter-day accuracy and precision were determined by analyzing QC samples on separate days against a calibration curve. Accuracy was expressed as percentage recovery and precision as relative standard deviation (R.S.D.) of replicate measurements.

The lower limit of quantitation (LLOQ) was defined as the lowest concentration that could be determined with accuracy within 80-120% and a precision < 20% on a day-to-day basis. To determine the analytical error in the LLOQ, spiked QC samples were used.

The matrix effect (i.e., suppression or enhancement of ionization of analytes by the presence of matrix components) was investigated by using six different batches of drug-free plasma by comparing peak areas of spiked samples with or without biological matrix at concentrations of QC samples (n = 3 replicates per QC). Matrix factor was defined as a ratio of the analyte peak response in the presence of matrix ions to the analyte peak response in the absence of matrix ions. Matrix factor values between 0.85-1.15 were judged acceptable.

The extraction efficiency of EAPB02303 and EAPB02302 from plasma was calculated by comparing peak areas of samples spiked before and after extraction at concentrations of QC samples ($n \geq 6$ replicates per QC).

Carryover was assessed by injecting blank sample after a high concentration sample or standard. Ruggedness testing was carried out with a standard solution containing 31.3 ng/mL of the two analytes in the mobile phase by performing small changes in LC-MS/MS conditions (age of columns, column temperature, pH of buffer, composition of the mobile phase, flow rate, temperature and mass spectrometer parameters). Ruggedness of the method was also evaluated by using different analysts and different lots of columns.

2.4.6. Dilution integrity

Dilution integrity was carried out to ensure the integrity of analytes in those samples which are beyond upper limit of the standard curve and need to be diluted. QC samples containing EAPB02303 and EAPB02302 at concentrations of 1250, 2500, 5000 and 10000 ng/mL were prepared. They were then diluted 2.5-, 5-, 10- and 20-fold with the same blank plasma, respectively. Three aliquots of each dilution were processed along with freshly spiked calibration standards and analyzed by back-calculation using regression equation obtained. The integrity of the samples was considered to be maintained if % recoveries are within ± 15% of nominal values and % R.S.Ds. ≤ 15% at all diluted levels.

2.4.7. Stability assays

The stability of EAPB02303 and EAPB02302 stock solutions was tested at the storage temperature of -20 °C after a six-month period, by comparing with freshly prepared stock solutions. The stability of EAPB02303 and EAPB02302 in rat and mice plasma including (i) three freeze-thaw cycles; (ii) storage for four months at -20 °C; (iii) storage for 72 h at 4 °C; and (iii) bench-top room temperature storage (20 °C) for 6 h was investigated by analyzing QC samples against freshly prepared calibration curves. Each determination was performed in triplicate. In addition, the stability of EAPB02303 and EAPB02302 was assessed at

concentrations of calibration curve in processed samples in the autosampler (72 h at 4 °C). A drug was considered stable if at least 85% of the intact drug was retained at the end of the study period.

2.5. Pharmacokinetic study

Male C57Bl/6 mice used in this study were from Janvier Labs. Mean body weight was 22.8 g at the study initiation. The minimum and maximum weight in the group was within a range of ± 20 % of the group mean. This research adhered to the "Principles of Laboratory Animal Care" (National Institutes of Health publication publication #85-23, revised 1985). The animal study was approved by the local Animal Use Committee.

Each mouse received a single intraperitoneal administration of 37.5 mg/kg of EAPB02303 dissolved in a mixture of DMSO, Tween 80 and sodium chloride solution 0.9% (10/10/80, v/v/v). Blood samples (one sample per mouse) were collected in heparinized polypropylene tubes at the following time-points (3 animals per time-point): 5, 10, 15, 30 min, and 1, 2, 4, 8, and 24 h after drug administration. Blood were sampled after sacrifice of the animal by section of the carotid artery. Before sampling, animals were anaesthetized with isoflurane. Blood samples were centrifuged at 4 °C (10 min at 4000g). Plasma samples were transferred into polypropylene tubes and immediately stored at -20 °C until assay.

The assay method described in 2.4 was used to quantify EAPB02303 and EAPB02302 in plasma samples drawn during this study.

Pharmacokinetic parameters (CL (total clearance); V_1 (central volume of distribution); Vss (steady-state volume of distribution); AUC (area under curve) and terminal half-life) were computed from the average concentration values at each time point using the NONMEM® software [28]. CL, V_1 and Vss were uncorrected for bioavailability (F).

3. Results and discussion

3.1. In vitro cytotoxic activity

Results are presented in Table 2. On the A375 human melanoma cancer cell line, EAPB02303 exhibits in vitro cytotoxic activity 6 times higher than vemurafenib, while similar cytotoxic activities are observed for EAPB02302 and vemurafenib. Interestingly, EAPB02303 shows an in vitro cytotoxic activity about 40 times higher than that of our first identified lead compound, EAPB0503 [13]. On the other hand, the in vitro cytotoxic activities of fotemustine and imiquimod, the drugs used as references in our previous studies, against A375 human melanoma cancer cell line are much lower with IC_{50} values of 173 and 70 µM, respectively [11].

3.2. MS/MS fragmentations of EAPB02303 and EAPB02302.

High resolution experiments were performed in both MS and MS/MS mode of acquisition in order to deduce the elemental compositions of the $[M+H]^+$ precursor ions and some of the observed fragment ions. The difference between the measured and the calculated exact masses was lower than 3 ppm which indicated relatively good mass accuracies (± 0.01 Th). QTof-MS/MS spectra of the $[M+H]^+$ precursor ions at *m/z* 307 (EAPB02303) and *m/z* 293 (EAPB02302) recorded at increasing collision energies are presented in Fig. 1A–B of the online Data Supplement , respectively.

At low collision energies, EAPB02303 shows predominant fragment ions at *m/z* 292/291 (resulting from the loss of $CH_3^{\bullet}$ (loss of 15 Da) / CH_4 (loss of 16 Da) from *m/z* 307) and *m/z* 278 (resulting from the loss of the imine $NHCH_2$ (loss of 29 Da) from *m/z* 307). Although the loss of a radical is scarcely observed with soft ionization techniques as electrospray ionization (ESI), which produce even electron ions, such behavior has been previously described for other compounds of the same chemical series [20-21] and was thus expected to occur since the loss

of $CH_3^{\bullet}$ radical give stable fragment radical cations as depicted in Fig. 2. Minor fragments are observed at *m/z* 265 (loss of the alkene C_2H_2 from *m/z* 291) via retro-Diels–Alder reactions and *m/z* 280 (loss of the nitrile CHN from *m/z* 307). A fragment ion at *m/z* 131, related to quinoxaline skeleton, is also observed giving *m/z* 104 by the consecutive loss of CHN (27 Da). The MS/MS spectrum recorded at 35 eV and the main fragmentation pathways are presented in Fig. 2. Increasing the collision energy provided more abundant low mass fragment ions. Fig. 1A-b of the online Data Supplement displayed all MS/MS spectra acquired with the QTof instrument.

In contrast, at the same collision energy of 35 eV, EAPB02302 shows predominant fragment ions only issued from small neutral losses such as CHN and H_2O to give, respectively, *m/z* 266 and *m/z* 275 (from $(M+H)^+$ at *m/z* 293). These ions underwent further dissociations to produce secondary fragments by the loss of CHN, H_2O, NH_3 and CO as displayed in Fig. 3. In this case, the loss of a radical only represented minor dissociation pathways with the corresponding fragment ions observed at *m/z* 292 (loss of $H^{\bullet}$) and *m/z* 276 (loss of $OH^{\bullet}$). Fragment ions at *m/z* 144 and 131 related to quinoxaline skeleton and at *m/z* 104 after the loss of CHN from *m/z* 131 are also observed. Fig. 1B-b of the online Data Supplement showed all MS/MS data acquired under various dissociation conditions.

The two different fragmentation patterns observed with EAPB02303 and EAPB02302 clearly show the specific implication of the C-N sigma bond in the generation of fragments. Actually, the initial loss of the CH3$^{\bullet}$ radical in EAPB02303 dramatically sensitizes the extranuclear C-N bond on position 4 of the heterocycle and induces specific patterns of secondary fragmentations in the near environment of the amino group.

3.3. Quantitation of EAPB02303 and EAPB02302 in rat and mouse plasma

3.3.1. Method development

In previous papers from our group [14,15,18], a solid-phase extraction procedure using Oasis HLB cartridge was used to quantify EAPB0203, EAPB0503 and their metabolites in rat plasma. This clean-up method gave good results but it was cost-effective due to material costs. Moreover, this method was not fully automated.

Organic precipitation and liquid-liquid extraction were then tested for sample preparation in this experiment. It was found that organic precipitation with acetonitrile, methanol or acetone did not provide the satisfactory recovery of EAPB02303 and EAPB02302. To achieve higher recovery and sensitivity as well as eliminating endogenous interferences, liquid-liquid extraction was undertaken. In an initial step, the most important parameters affecting both extraction and clean-up efficiencies were optimized. The following parameters were included in this screening design: i) the acid used to precipitate proteins before extraction (formic acid or trifluoroacetic acid), and ii) the type of solvents (ethyl acetate, dichloromethane, chlorobutane) to extract the analytes from the matrix. Finally, better recoveries for EAPB02303 and EAPB02302 were achieved by adding 1% formic acid in the extraction solution and conducting the extraction with ethyl acetate. In a second step, the best conditions were slightly modified to obtain a good selectivity in regard to endogenous compounds from the matrix. Different internal standards from this new group of compounds were also checked. Thus, EAPB0602 was chosen as internal standard because of its similar structure, physiochemical properties and mass spectrometric behavior compared to those of EAPB02303 and EAPB02302. In addition, there was no interference at the retention time of this compound. Chromatographic conditions were optimized to improve peak shape, increase signal response of analytes and shorten run time. This included column type (C8 Zorbax Eclipse XDB, C18 RP18 Nucleoshell, C18HD nucleosil, ODS Hypersil, and EVO Kinetex), composition of the mobile phase, pH of buffer solution and flow rate. The presence of organic acid (formic, acetic, or trifluoroacetic acid) or buffer (formate or acetate) in the mobile phase was evaluated.

For all analytes the signals obtained in positive mode had much higher intensities than those obtained in negative mode. To optimize MS parameters, preliminary tuning experiments were carried out via direct infusion into the mass spectrometer of a standard solution containing 5000 ng/mL of EAPB02303, EAPB02302 and IS dissolved in the mobile phase. The most intense transitions $[M+H]^+$ at m/z 307 → 292 for EAPB02303, m/z 293 → 104 for EAPB02302 and m/z 277 → 177 for EAPB0602 were used as a quantifier; the other transitions were used as qualifier.

This optimization procedure has led to the optimal experimental conditions described in 2.4.4.

3.3.2. Validation results

EAPB02303 and EAPB02302 eluted at retention times (rt) of 1.87 ± 0.03 min and 1.74 ± 0.02 min (n = 48), respectively. The six different lots of rat and mouse plasma, commercially procured, were chromatographically screened for interfering substances and did not show significant interference at the retention times of the analytes. Representative MRM chromatograms of the blank rat plasma and blank rat plasma spiked with EAPB02303 and EAPB02302 at two concentrations (LLOQ and 1000 ng/mL) and internal standard may be found in Fig. 2 of the online Data Supplement. Chromatograms of a blank mouse plasma, a blank mouse plasma spiked with EAPB02303 and EAPB02302 at the LLOQ and internal standard (EAPB0602) at 125 ng/mL, and a plasma sample from a mouse 10 min after treatment with EAPB02303 (37.5 mg/kg) are presented in Fig. 4.

In rat plasma, the method was validated over the range 1.95-1000 ng/mL for EAPB02303 and 7.81-1000 ng/mL for EAPB02302. In mouse plasma, the calibration ranges were 0.98-1000 ng/mL and 1.95-1000 ng/mL for the two analytes, respectively. Based on the analysis of residuals and the acceptance criteria [24-26] of the concomitant QC samples calculated

according the different models applied to a particular calibration set, the best fit for the standard curves was obtained using an unweighted quadratic function. The R.S.D. values on the slope were below 15%. Mean parameters are presented in Table 3. Variations in back-calculated concentrations (given as R.S.D. (%)) of all calibration curves ranged from 0.49 to 6.17% for EAPB02303 and from 1.82 to 8.78% for EAPB02302; the mean bias between back-calculated and nominal concentrations were between −5.4 to 2.8% for EAPB02303 and between −2.9 to 5.2% for EAPB02302. Results are presented in Tables 1 (rat plasma) and 2 (mouse plasma) of the online Data Supplement. The goodness of fit between back-calculated concentrations and introduced concentrations was statistically verified (Student's t-test). The mean relative predictor error calculated from the difference between back-calculated and nominal concentrations was not statistically different from zero. The 95% confidence intervals in rat plasma were −1.55;1.48 for EAPB02303 and −1.71;2.24 for EAPB02302. In mouse plasma, they were −4.02;4.18 for EAPB02303 and −1.86;1.70 for EAPB02302. Distributions of residuals are presented in Fig. 3 of the online Data Supplement.

Precision and accuracy complied with the FDA and EMA recommendations [24-26]. The upper concentration limits can be extended to 10000 ng/mL. The mean back-calculated concentrations for 1/20, 1/10, 1/5 and 1/2.5 dilution samples were within 90.6-103.6% of their nominal values. Results are reported in Table 4.

For EAPB02303, extraction recoveries were 98.9% (R.S.D., 9.0%) in rat plasma and 93.3% (R.S.D., 6.4%) in mouse plasma. They were 99.4% (R.S.D., 8.1%,) and 96.8% (R.S.D., 10.0%) for EAPB02302, and 98.2% (R.S.D., 5.3%) and 96.9% (R.S.D., 8.1%) for the internal standard in rat and mouse plasma, respectively. These recoveries were not statistically different over the range of concentrations studied.

In rat plasma, the LLOQs were 1.95 ng/mL for EAPB02303 and 7.81 ng/mL for EAPB02302. In mouse plasma, they were 0.98 ng/mL and 1.95 ng/mL for the two analytes,

respectively. At these levels, the precision of determination, expressed as R.S.D. was < 8.2% with adequate assay accuracy (96.8-103.7%).

The mean matrix factors in rat plasma ranged from 98.3% to 104.0% (R.S.D. ≤ 6.9%) for EAPB02303 and from 91.8% to 108.5% (R.S.D. ≤ 8.8%) for EAPB02302. In mouse plasma, they ranged from 90.4% to 102.4% (R.S.D. ≤ 7.6%) and from 90.4% to 98.2% (R.S.D. ≤ 7.3%) for EAPB02303 and EAPB020302, respectively. Moreover, no suppression/enhancement for the internal standard could be detected when compound in neat injection solvent was compared with compound in extracted blank biological matrix (107.8% (R.S.D., 4.2%) in rat plasma; 102.5% (R.S.D., 3.8%) in mouse plasma).

In this analysis no quantifiable carryover effect was observed when a series of blank plasma solutions were injected immediately following the highest calibration standard.

The results indicated that small changes in the LC-MS/MS conditions did not have significant effect on the determination of EAPB02303 and EAPB02302.

3.3.3. Stability

Stock solutions of EAPB02303 and EAPB02302 were stable at −20 °C for up to 6 months.

In rat and mouse plasma, stored at −20 °C, EAPB02303 and EAPB02302 at the concentrations of QC samples were stable for at least 4 months. After bench-top storage at room temperature for 6 h, recoveries were > 87.8% for EAPB02303 and EAPB02302**.** Stored at 4 °C for 3 days, recoveries were > 92% for EAPB02303; and > 91% for EAPB02302. Reconstituted extracts in the mobile phase were stable in the autosampler at 4 °C for 48 h. Three freeze-thaw cycles did not affect the stability of EAPB02303 and EAPB02302.

3.4. Pharmacokinetic study

This developed and validated LC-MS/MS method was used to quantify EAPB02303 and EAPB02302 in mouse plasma drawn during a pharmacokinetic study performed in C57Bl/6 mice. Semilogarithmic plot of the mean (±SD) EAPB02303 plasma concentration-time profile is presented in Fig. 5. EAPB02303 plasma concentrations decline in a biphasic manner. We can observe that EAPB02303 plasma concentrations remain greater than 4-fold the IC_{50} value against A375 cell line for more than 8 h following administration. After intraperitoneal administration, the peak plasma concentration was obtained in 10 minutes following administration. These data suggest that EAPB02303 is rapidly absorbed from the peritoneal fluid into the blood compartment. Pharmacokinetic parameters are as follows: CL/F, 33.4 L/h/kg; V_1/F, 6.26 L/kg; Vss/F, 51.9 L/kg; AUC, 1,122.8 µgxh/L; and terminal half-life, 6.11 h.

EAPB02302 was not detected in plasma. Thus, unlike EAPB0203 and EAPB0503, the first two lead compounds, the *N*-demethylation of EAPB02303 does not appear to be a metabolic pathway in mice.

4. Conclusion

Since several years, our group is particularly involved in the study and development of new imidazo[1,2-*a*]quinoxaline compounds [8-10,29]. Two compounds, EAPB0203 and EAPB0503, were first identified as lead compounds due to their interesting antitumoral activities against a variety of tumors, particularly on the melanoma. The modulation of the chemical structure of these compounds has led to the synthesis of EAPB02303 and EAPB02302 exhibiting a significant increase of the in vitro cytotoxic activity. Thus, before to perform an in vivo activity study in a xenograft mouse model, a sensitive, specific, and reproducible LC-MS/MS method was developed and validated for the simultaneous analysis of these compounds in rat and mouse plasma. The assay showed excellent intra- and inter-day precision and

accuracy. The levels of quantification were 1.95 ng/mL for EAPB02303 and 7.81 ng/mL for EAPB02302 in rat plasma, and 0.98 ng/mL and 1.95 ng/mL for the two compounds in mouse plasma, respectively with %R.S.D. and bias values both considerably below the +/- 20% criteria. This method was successfully applied to the determination of EAPB02303 in male C57Bl/6 mouse plasma after single intraperitoneal administration of 37.5 mg/kg. The *N*-demethylation of EAPB02303 does not appear to be a metabolic pathway in mice. The pharmacokinetic parameters calculated during this study will be used to determine the doses and rhythm of administration during the future preclinical activity studies.

Financial disclosures

Non applicable

Acknowledgments

The authors wish to thank the Société d'Accélération du Transfert de Technologie AxLR (Montpellier, France) for its financial support and 4P-Pharma (Lille, France) for its technical support.

Appendix A. Supplementary data associated with this article can be found, in the online version, at http://.

References

[1] W.B. Grant, Critique of the International Agency for Research on Cancer's meta-analyses of the association of sunbed use with risk of cutaneous malignant melanoma, Dermato endocrinol. 1 (2009) 294–299.

[2] F. Erdmann, J. Lortet-Tieulent, J. Schüz, H. Zeeb, R. Greinert, E.W. Breitbart, F. Bray, International trends in the incidence of malignant melanoma 1953-2008--are recent generations at higher or lower risk?, Int. J. Cancer. 132 (2013) 385–400.

[3] S.C. Azoury, J.R. Lange, Epidemiology, risk factors, prevention, and early detection of melanoma, Surg. Clin. North Am. 94 (2014) 945–962.

[4] J.E. Russak, D.S. Rigel, Risk factors for the development of primary cutaneous melanoma, Dermatol. Clin. 30 (2012) 363–368.

[5] R. Dummer, A. Hauschild, N. Lindenblatt, G. Pentheroudakis, U. Keilholz, ESMO Guidelines Committee, Cutaneous melanoma: ESMO Clinical Practice Guidelines for diagnosis, treatment and follow-up, Ann. Oncol. Off. J. Eur. Soc. Med. Oncol. 26 Suppl 5 (2015) v126-132.

[6] Pereira JA, Pessoa AM, Cordeiro MNDS, Fernandes R, Prudêncio C, Noronha JP, et al. Quinoxaline, its derivatives and applications: A State of the Art review. Eur J Med Chem. 97 (2015) 664–672.

[7] Mamedov VA, Kalinin AA. Advances in the synthesis of imidazo[1,5-a]- and imidazo[1,2-*a*]quinoxalines. Russ Chem Rev. 83 (9) (2014) 820.

[8] C. Deleuze-Masquefa, G. Moarbess, P.A. Bonnet, F. Pinguet, A. Bazarbachi, F. Bressolle, Imidazo[1,2-*a*]quinoxalines et dérivés pour le traitement des cancers. WO2009043934 A1 (2009).

[9] C. Deleuze-Masquefa, G. Moarbess, P.A. Bonnet, F. Pinguet, A. Bazarbachi, F. Bressolle. Patent US 20138378098 B2 (2013).

[10] C. Deleuze-Masquefa, G. Moarbess, P.A. Bonnet, F. Pinguet, A. Bazarbachi, F. Bressolle. Canadian Patent 2 701 386 (2016).

[11] G. Moarbess, C. Deleuze-Masquéfa, V. Bonnard, S. Paniagua, J.R. Vidal, F. Bressolle, F. Pinguet, P.A. Bonnet, In vitro and in vivo antitumoral activities of imidazo[1,2-*a*]quinoxaline, imidazo[1,5-*a*]quinoxaline, and pyrazolo[1,5-*a*]quinoxaline derivatives, Bioorg. Med. Chem. 16 (2008) 6601–6610.

[12] G. Moarbess, H. El-Hajj, Y. Kfoury, M.E. El-Sabban, Y. Lepelletier, O. Hermine, C. Deleuze-Masquéfa, P.A. Bonnet, A. Bazarbachi, EAPB0203, a member of the imidazoquinoxaline family, inhibits growth and induces caspase dependent apoptosis in T cell lymphomas and HTLV-I associated adult T-cell leukemia/lymphoma, Blood 111 (2008) 3770–3777.

[13] C. Deleuze-Masquéfa, G. Moarbess, S. Khier, N. David, S. Gayraud-Paniagua, F. Bressolle, F. Pinguet, P.A. Bonnet, New imidazo[1,2-*a*]quinoxaline derivatives synthesis and in vitro activity against human melanoma, Eur. J. Med. Chem. 44(2009) 3406–3411.

[14] S. Khier, G. Moarbess, C. Deleuze-Masquéfa, D. Margout, I. Solassol, F. Pinguet, P.A. Bonnet, F.M.M. Bressolle, Quantitation of two imidazo[1,2-*a*]quinoxaline derivatives (EAPB0503 and EAPB0603) with anti-tumoral activity in human and rat plasma by liquid chromatography-electrospray mass spectrometry. Application to a Pharmacokinetic Study, J. Sep. Sci. 32 (2009) 1363–1373.

[15] S. Khier, C. Deleuze-Masquéfa, G. Moarbess, F. Gattacceca, D. Margout, I. Solassol, J.F. Cooper, F. Pinguet, P.A. Bonnet, F.M.M. Bressolle, Pharmacology of EAPB0203, a novel imidazo[1,2-*a*]quinoxaline derivative with anti-tumoral activity on melanoma, Eur. J. Pharm. Sci. 39 (2010) 23–29.

[16] J. Saliba, C. Deleuze-Masquéfa, A. Iskandarani, R. El Eit, R. Hmadi, F.-X. Mahon, A. Bazarbachi, P.A. Bonnet, R. Nasr, EAPB0503, a novel imidazoquinoxaline derivative,

inhibits growth and induces apoptosis in chronic myeloid leukemia cells, Anticancer. Drugs. 25 (2014) 624–632.

[17] A.I. Nabbouh, R.S. Hleihel, J.L. Saliba, M.M. Karam, M.H. Hamie, H.-C.J.M. Wu, C.P. Berthier, N.M. Tawil, P.A. Bonnet, C. Deleuze-Masquefa, H.A. El Hajj, Imidazoquinoxaline derivative EAPB0503: A promising drug targeting mutant nucleophosmin 1 in acute myeloid leukemia, Cancer (2017) Jan 5. doi: 10.1002/cncr.30515.

[18] S. Khier, F. Gattacceca, S. El Messaoudi, F. Lafaille, C. Deleuze-Masquéfa, J. Bompart, J.F. Cooper, I. Solassol, F. Pinguet, P.A. Bonnet, F.M.M. Bressolle, Metabolism and pharmacokinetics of EAPB0203 and EAPB0503, two imidazoquinoxaline compounds previously shown to have anti-tumoral activity on melanoma and T-lymphomas, Drug Metab. Dispos. 38 (2010) 1836–1847.

[19] Z. Zghaib, J.F. Guichou, J. Vappiani, N. Bec, K. Hadj-Kaddour, L.A. Vincent, S. Paniagua-Gayraud, C. Larroque, G. Moarbess, P. Cuq, I. Kassab, C. Deleuze-Masquéfa, M. Diab-Assaf, P.A. Bonnet, New imidazoquinoxaline derivatives: Synthesis, biological evaluation on melanoma, effect on tubulin polymerization and structure-activity relationships. Bioorg. Med. Chem. 24 (2016) 2433-40.

[20] F. Lafaille, B. Banaigs, N. Inguimbert, C. Enjalbal, P.E. Doulain, P.A. Bonnet, C. Masquefa, F.M.M. Bressolle, Characterization of a new anticancer agent, EAPB0203 and its main metabolites: nuclear magnetic resonance and liquid chromatography-mass spectrometry studies, Anal. Chem. 84 (2012) 9865–9872.

[21] F. Lafaille, I. Solassol, C. Enjalbal, B. Bertrand, P.E. Doulain, J. Vappiani, P.A. Bonnet, C. Deleuze-Masquéfa, F.M. Bressolle. Structural characterization of in vitro metabolites of the new anticancer agent EAPB0503 by liquid chromatography-tandem mass spectrometry, J. Pharm. Biomed. Anal. 88 (2014) 429-40.

[22] P. Cuq, C. Deleuze-Masquefa, P.-A. Bonnet, C. Patinotte, Nouveaux imidazo[1,2-*a*]quinoxalines et dérivés pour le traitement des cancers. WO2016107895 A1 (2016).

[23] G. Kim, A.E. McKee, Y.M. Ning, M. Hazarika, M. Theoret, J.R. Johnson, Q.C. Xu, S. Tang, R. Sridhara, X. Jiang, K. He, D. Roscoe, W.D. McGuinn, W.S. Helms, A.M. Russell, S.P. Miksinski, J.F. Zirkelbach, J. Earp, Q. Liu, A. Ibrahim, R. Justice, R. Pazdur, FDA approval summary: vemurafenib for treatment of unresectable or metastatic melanoma with the BRAFV600E mutation, Clin. Cancer Res. 20 (2014) 4994-5000.

[24] G. Tiwari, R. Tiwari, Bioanalytical method validation: an updated review, Pharm. Methods 1 (2010) 25–38.

[25] C.T. Viswanathan, S. Bansal, B. Booth, A.J. DeStefano, M.J. Rose, J. Sailstad, V.P.Shah, J.P. Skelly, P.G. Swann, R. Weiner, Quantitative bioanalytical methods validation and implementation: best practices for chromatographic and ligand binding assays, Pharm. Res. 24 (2007) 1962–1973.

[26] European Medicines Agency Guideline on Bioanalytical Method Validation., 2011 http://www.ema.europa.eu/docs/enGB/documentlibrary/Scientificguideline/2011/08/WC500109686.pdf.

[27] A. Cappiello, G. Famiglini, P. Palma, E. Pierini, V. Termopoli, H. Trufelli, Overcoming matrix effects in liquid chromatography-mass spectrometry, Anal. Chem. 80 (2008) 9343–9348.

[28] Beal S, Sheiner LB, Boeckmann A, Bauer RJ (2009). NONMEM User's Guides. (1989-2009), Icon Development Solutions. Ellicott City: MD, USAMD, USA.

[29] C. Patinote, K. Hadj-Kaddour, M. Damian, C. Deleuze-Masquéfa, P. Cuq, P.-A. Bonnet, Fluorescence Study of Imidazoquinoxalines, J. Fluoresc. (2017). doi:10.1007/s10895-017-2097-z.

Figure Legends

Fig. 1. Structural formulas of EAPB02302, EAPB02303 and EAPB0602 (internal standard).

Fig. 2. MS/MS spectra of EAPB02303 recorded with the QTof instrument at collision energy of 35 keV (A) and proposed fragmentation pathways (B).

Fig. 3. MS/MS spectra of EAPB02302 recorded with the QTof instrument at collision energy of 35 keV (A) and proposed fragmentation pathways (B).

Fig. 4. Representative MRM chromatograms of (A) blank mouse plasma; (B) blank mouse plasma spiked with EAPB02303 and EAPB02302 at the LLOQ; and (C) mouse plasma sample collected 10 min after EAPB02303 intraperitoneal administration of 37.5 mg/kg, this sample has been diluted to 1/5 before analysis, concentration 3100 ng/mL.

Fig. 5. Mean ± SD plasma concentration-time profile of EAPB02303 in male C57Bl/6 mice after intraperitoneal administration of 37.5 mg/kg.

Table 1

Multiple reaction monitoring transitions selected for quantitation and optimal compound dependent MS/MS parameters.

	Quadrupole 1 (m/z)	Quadrupole 2 (m/z)	DP (V)	FP (V)	CE (eV)	CXP (V)
EAPB02303	307	292	61	250	41	16
EAPB02302	293	104	61	240	63	6
EAPB0602 (IS)	277	117	51	210	57	8

Quadrupole 1 was set to transmit the molecular ion and quadrupole 2 to transmit the product ions. DP, declustering potential; FP, focusing potential; CE, collision energy; CXP, collision cell exit potential.

Table 2

IC_{50} values against A375 human melanoma cancer cell line obtained in six replicates.

	IC_{50} (nM)
EAPB02303	10
EAPB02302	60
Vemurafenib	63
EAPB0503	383

IC_{50}, concentration of the compound producing 50% cell growth inhibition after 96 h of drug exposure, as determined by the MTT assay; SD, standard deviation.

Table 3

Mean parameters of the quadratic equation ($Y = aX^2 + bX + c$).

	EAPB02302	**EAPB02303**
	Rat plasma	
Within day (n = 6)		
a	6.15×10^{-7}	1.52×10^{-6}
b	4.87×10^{-3} (6.3%)	1.53×10^{-2} (7.9%)
c	2.91×10^{-3}	1.00×10^{-2}
Between-day (n = 14)		
a	3.69×10^{-7}	1.12×10^{-7}
b	4.19×10^{-3} (14.4%)	1.39×10^{-2} (9.1%)
c	6.80×10^{-4}	8.81×10^{-3}
	Mouse plasma	
Between-day (n = 6)		
a	-6.00×10^{-8}	-7.01×10^{-7}
b	4.15×10^{-3} (7.6%)	1.36×10^{-2} (12.9%)
c	8.57×10^{-4}	2.95×10^{-3}

R.S.Ds are given between parentheses.

Table 4

Intra- and inter-assay precision and accuracy results.

Nominal concentrations (ng/mL)	Precision, % (Recovery, %)	
	EAPB02302	**EAPB02303**
	Rat plasma	
Intra-day (n = 6)		
3.91	-	4.09 (102.3)
11.7	3.36 (103.4)	-
46.9	4.23 (104.3)	5.09 (102.3)
187	4.08 (103.4)	2.33 (102.0)
750	1.85 (101.3)	4.18 (98.8)
Inter-day (n = 37)		
3.91	-	7.18 (99.5)
11.7	5.98 (100.2)	-
46.9	4.99 (100.6)	4.55 (98.2)
187	6.33 (98.4)	5.55 (101.2)
750	6.25 (96.4)	4.79 (99.9)
Dilution integrity (n=3)		
10000	8.21 (100.8)	1.28 (90.6)
5000	4.61 (102.9)	12.5 (103.6)
2500	7.95 (97.0)	2.02 (93.1)
1250	6.14 (95.0)	1.83 (97.1)
	Mouse plasma	
Inter-day (n = 9)		
1.95	-	5.39 (98.7)
3.91	5.95 (100.6)	3.87 (99.8)
11.7	5.07 (99.4)	-
46.9	3.02 (98.2)	4.47 (102.5)
187	4.75 (95.9)	2.66 (98.7)
750	3.29 (99.3)	3.50 (101.3)

Fig. 1.

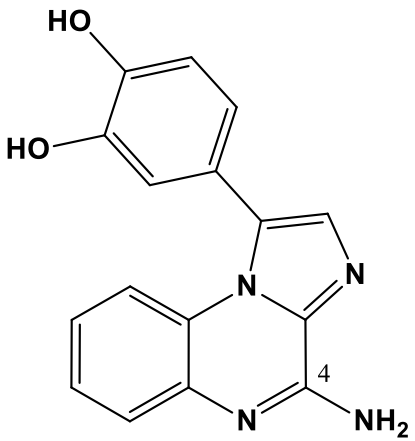

EAPB02302

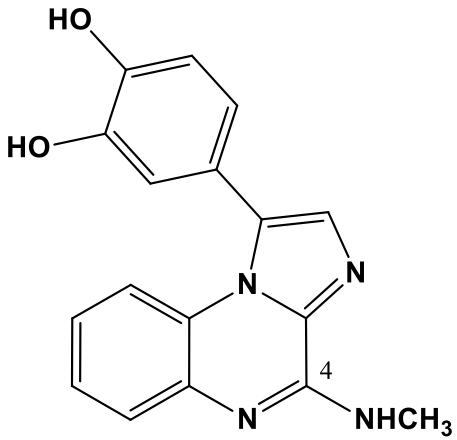

EAPB02303

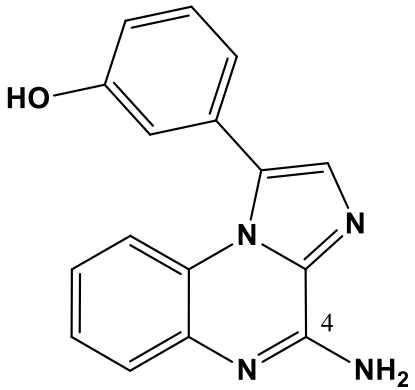

EAPB0602

Fig. 2.

A

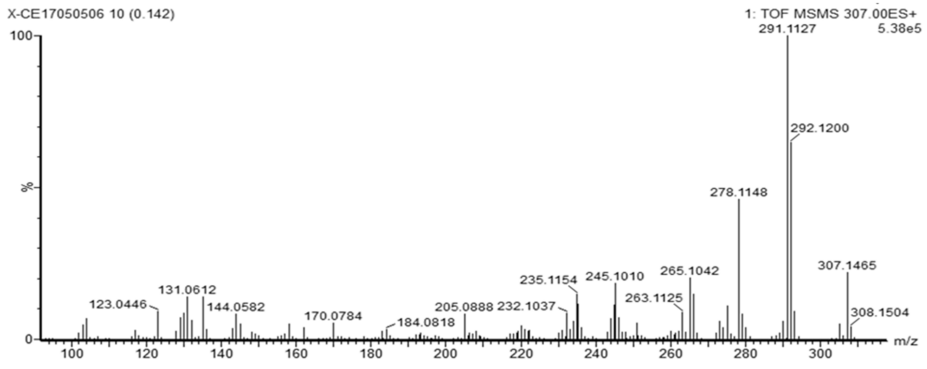
X-CE17050506 10 (0.142)
1: TOF MSMS 307.00ES+
291.1127
5.38e5
292.1200
278.1148
307.1465
265.1042
235.1154
245.1010
263.1125
131.0612
123.0446
144.0582
170.0784
205.0888
232.1037
184.0818
308.1504
%
m/z

B

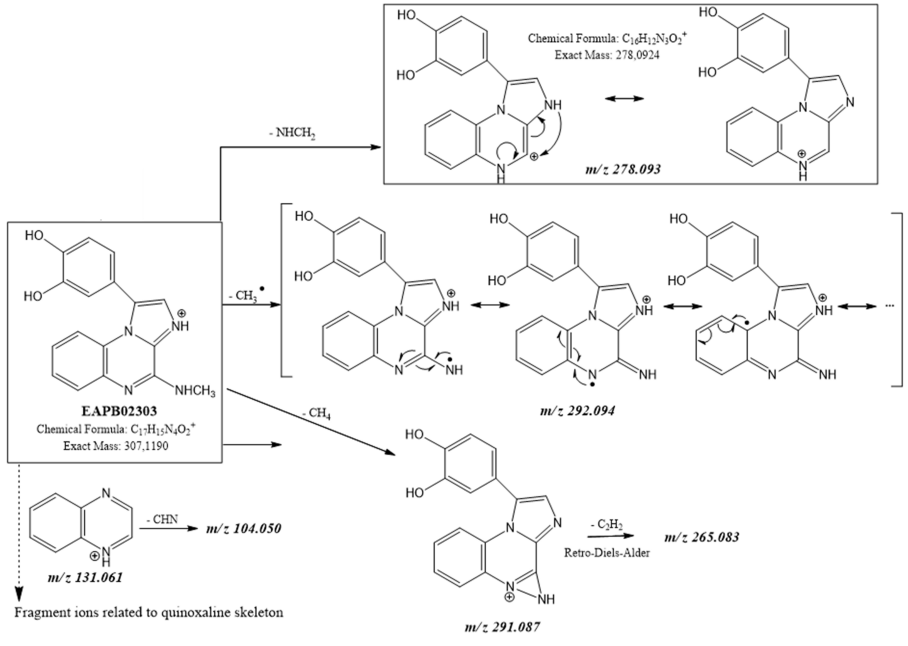
Chemical Formula: $C_{16}H_{12}N_3O_2^+$
Exact Mass: 278,0924
m/z 278.093
- NHCH$_2$
- CH$_3^\bullet$
EAPB02303
Chemical Formula: $C_{17}H_{15}N_4O_2^+$
Exact Mass: 307,1190
m/z 292.094
- CH$_4$
- CHN
m/z 104.050
m/z 131.061
- C$_2$H$_2$
Retro-Diels-Alder
m/z 265.083
m/z 291.087
Fragment ions related to quinoxaline skeleton

Fig. 3.

A

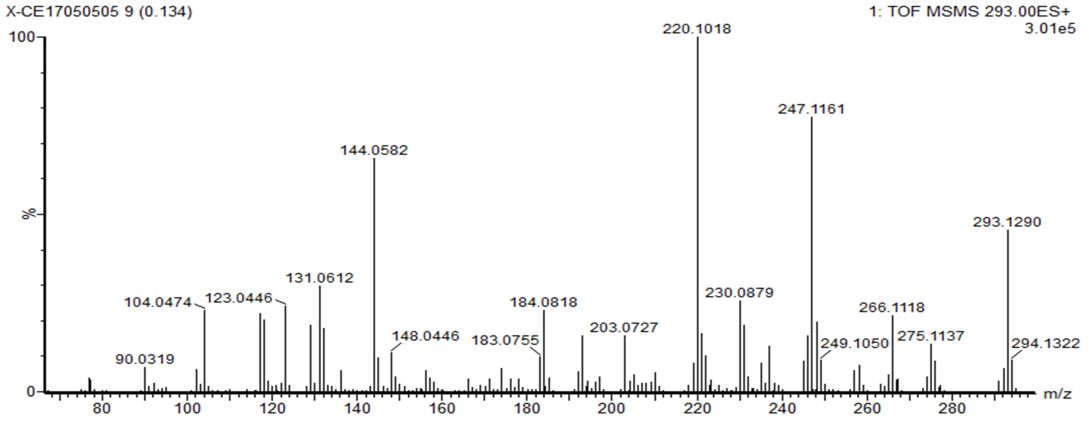

B

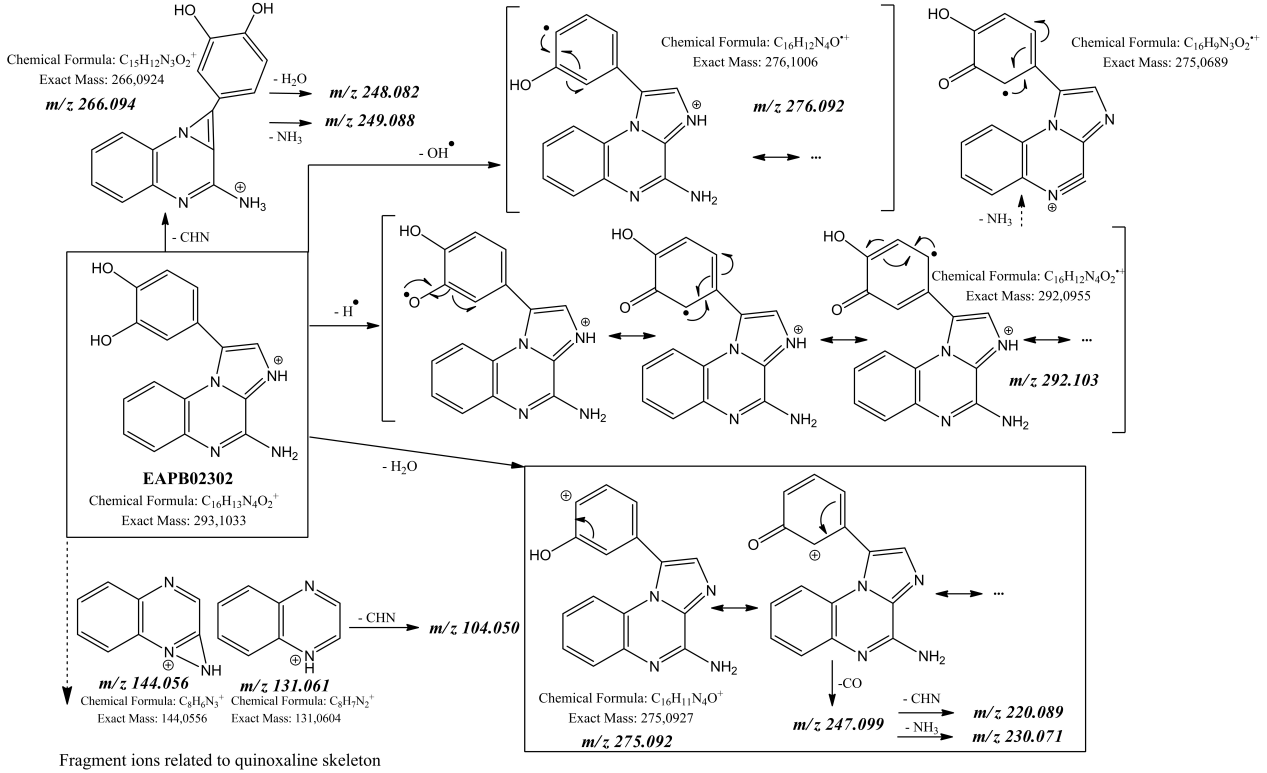

Fragment ions related to quinoxaline skeleton

Fig. 4

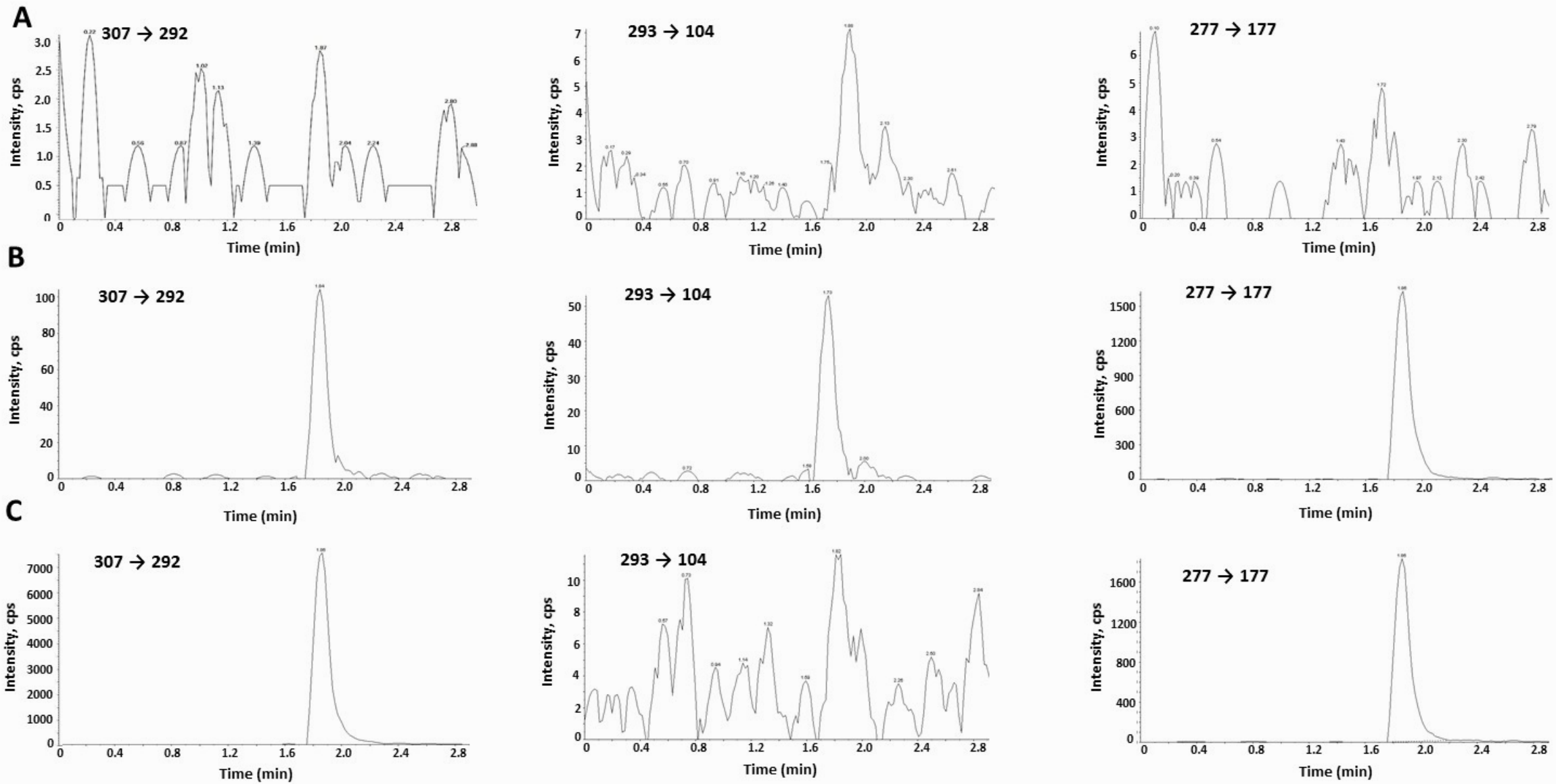
A
307 → 292
293 → 104
277 → 177
B
307 → 292
293 → 104
277 → 177
C
307 → 292
293 → 104
277 → 177
Intensity, cps
Time (min)

Fig. 5.

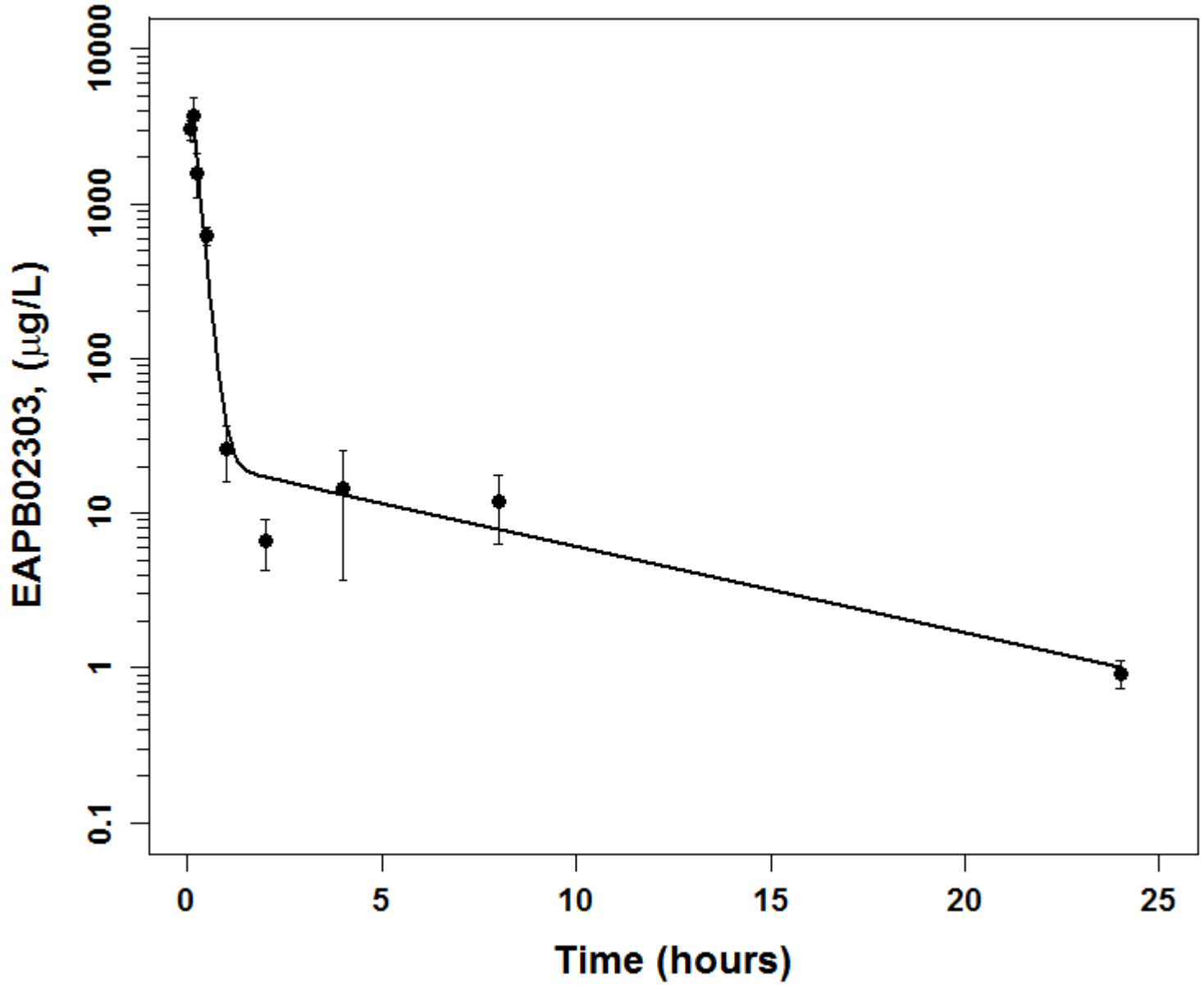

Supplemental Table 1

R.S.D.s and recoveries, calculated from back calculated concentrations, from calibration curves performed in rat plasma.

Nominal concentrations (ng/mL)	R.S.Ds, % (Recovery, %)	
	EAPB02302	**EAPB02303**
Within day (n = 6)		
1.95	_	0.77 (100.7)
7.81	6.27 (97.1)	4.51 (97.0)
15.6	6.82 (98.9)	5.67 (94.6)
31.2	6.12 (99.0)	2.80 (97.5)
62.5	8.78 (99.4)	4.95 (102.8)
125	2.27 (98.9)	4.69 (101.1)
250	2.03 (105.2)	3.07 (99.9)
500	3.35 (103.2)	2.04 (101.1)
1000	1.82 (97.7)	0.49 (99.3)
Between-day (n = 14)		
1.95	_	3.65 (99.4)
7.81	2.54 (101.5)	6.17 (99.1)
15.6	5.82 (97.3)	4.33 (99.7)
31.2	5.40 (97.3)	4.66 (100.4)
62.5	4.92 (104.0)	4.82 (99.7)
125	4.12 (100.3)	6.15 (98.8)
250	4.40 (98.5)	4.89 (100.4)
500	4.41 (101.2)	3.71 (101.2)
1000	2.40 (99.7)	2.66 (99.6)

Supplemental Table 2

R.S.D.s and recoveries, calculated from back calculated concentrations, from calibration curves performed in mouse plasma.

Nominal concentrations (ng/mL)	R.S.Ds, % (Recovery, %)	
	EAPB02302	**EAPB02303**
Between-day (n = 6)		
0.98	_	0.37 (99.8)
1.95	1.93 (99.0)	_
7.81	6.91 (100.9)	3.39 (100.8)
15.6	8.19 (103.7)	1.03 (99.6)
31.2	4.33 (98.9)	1.81 (102.0)
62.5	4.17 (97.6)	1.76 (100.8)
125	5.18 (99.0)	3.69 (100.2)
250	3.65 (99.2)	2.83 (96.8)
500	4.57 (97.3)	1.87 (98.4)
1000	3.40 (101.9)	0.84 (101.3)

Supplemental Fig. 1A: MS/MS spectra of EAPB2303.

a) recorded with the QqQ (API 3000 tandem triple quadrupole MS) instrument

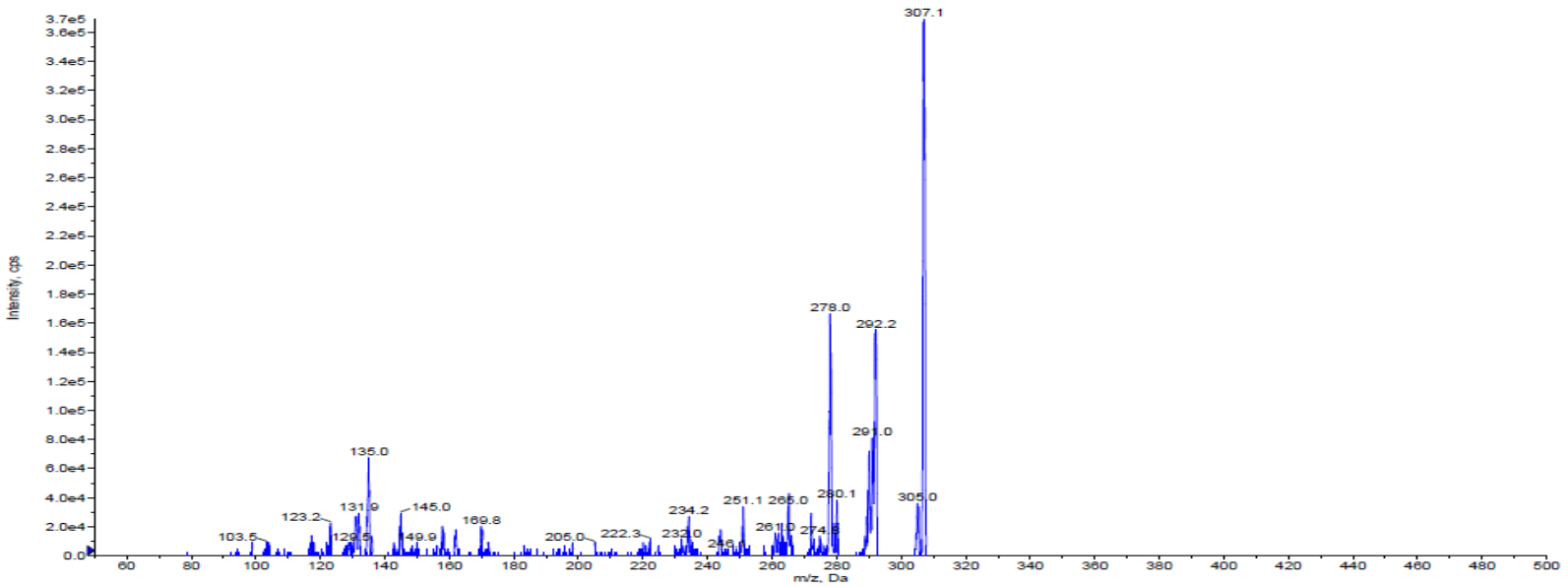

b) recorded with the QTof instrument at decreasing Collision Energy (CE)

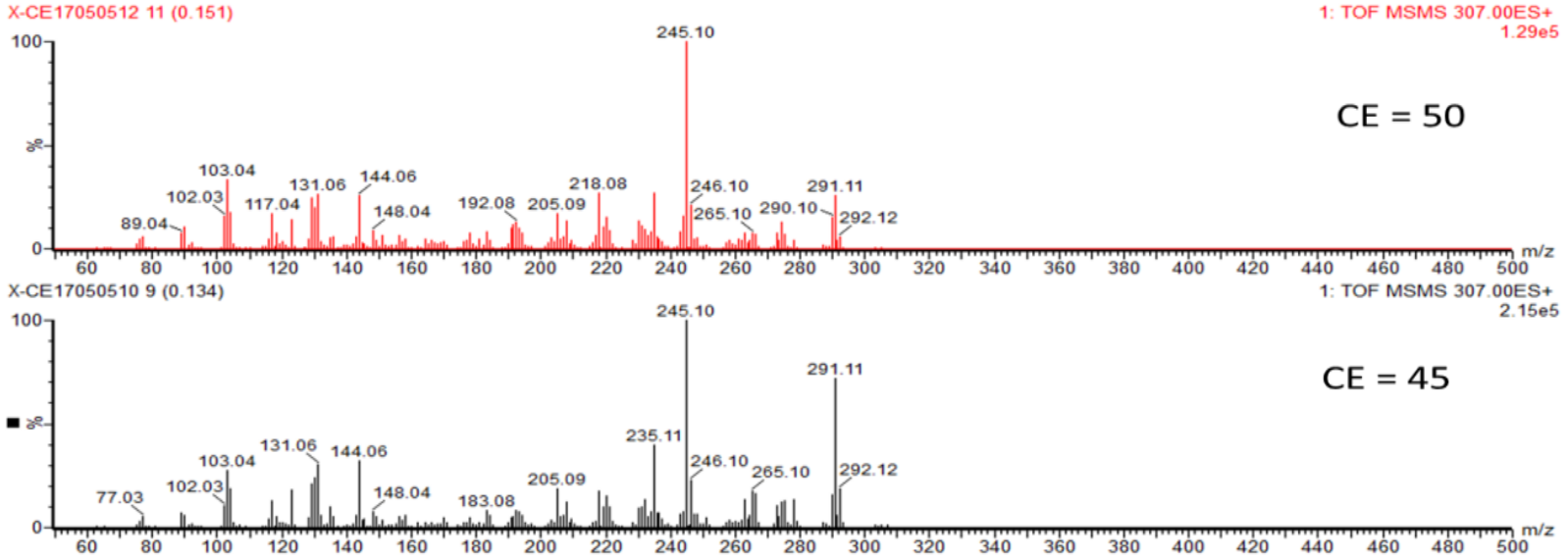

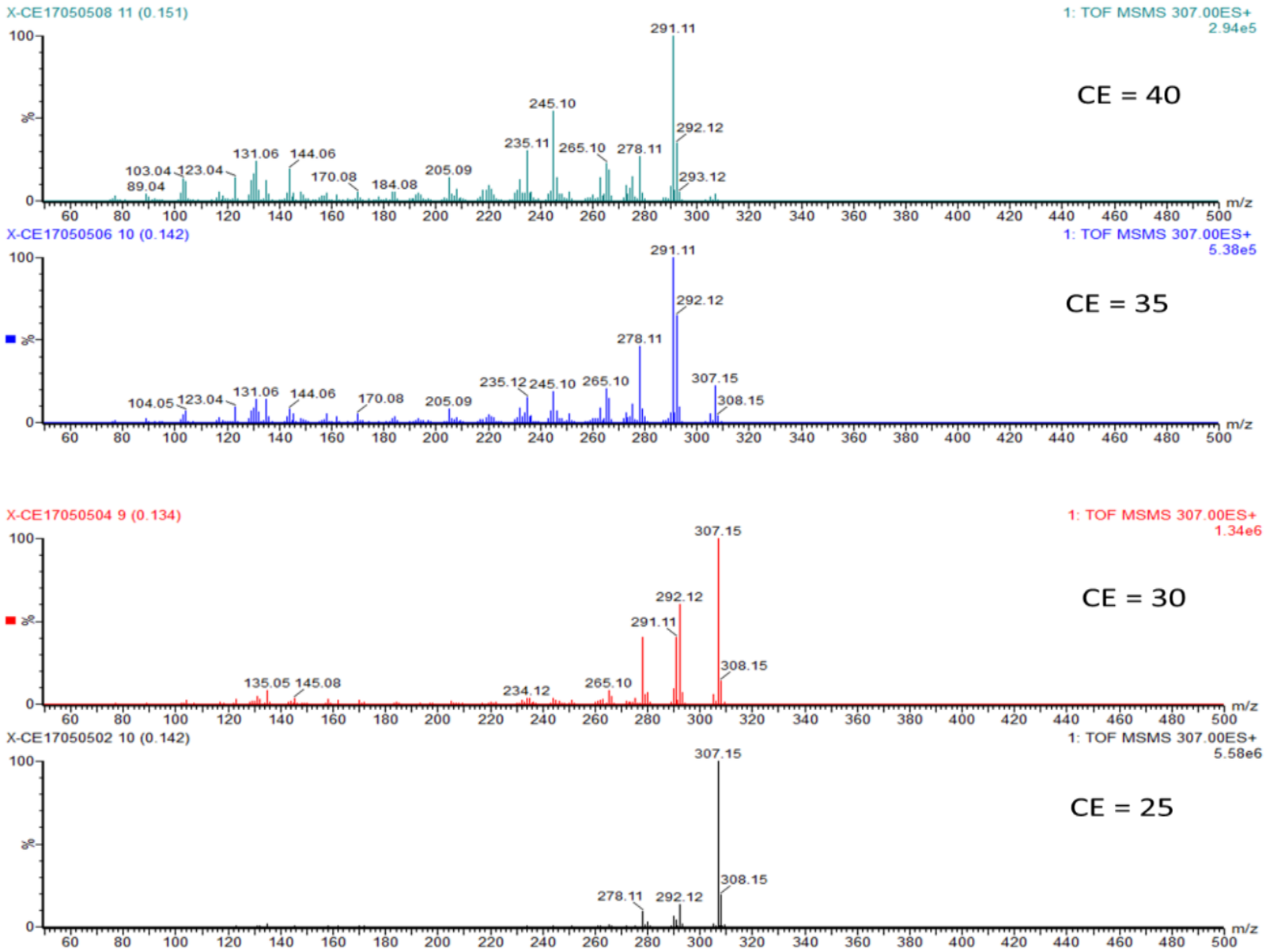
X-CE17050508 11 (0.151)
1: TOF MSMS 307.00ES+
2.94e5
CE = 40
291.11
245.10
292.12
235.11
265.10
278.11
131.06
144.06
103.04
123.04
293.12
170.08
184.08
205.09
89.04
X-CE17050506 10 (0.142)
1: TOF MSMS 307.00ES+
5.38e5
CE = 35
291.11
292.12
278.11
307.15
235.12
245.10
265.10
131.06
144.06
104.05
123.04
170.08
205.09
308.15
X-CE17050504 9 (0.134)
1: TOF MSMS 307.00ES+
1.34e6
CE = 30
307.15
292.12
291.11
308.15
135.05
145.08
234.12
265.10
X-CE17050502 10 (0.142)
1: TOF MSMS 307.00ES+
5.58e6
CE = 25
307.15
308.15
278.11
292.12
%
m/z

Supplemental Fig. 1B: MS/MS spectra of EAPB2302.

a) recorded with the QqQ (API 3000 tandem triple quadrupole MS) instrument

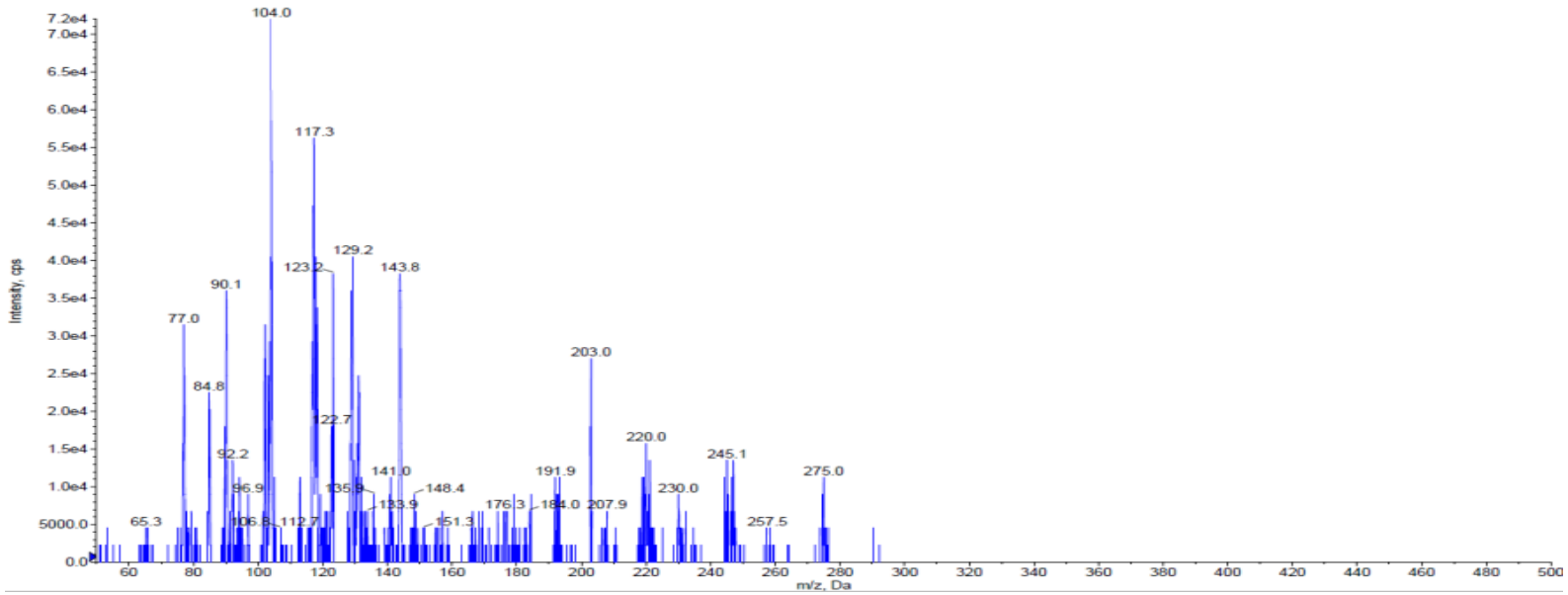

b) recorded with the QTof instrument at decreasing Collision Energy (CE)

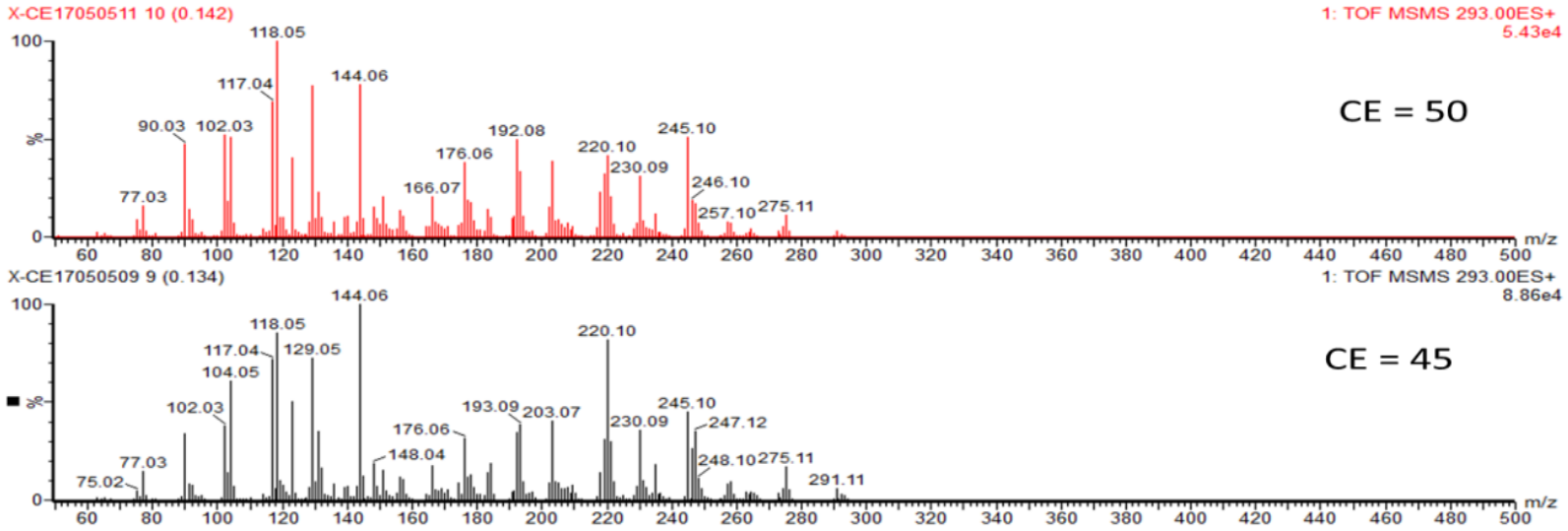

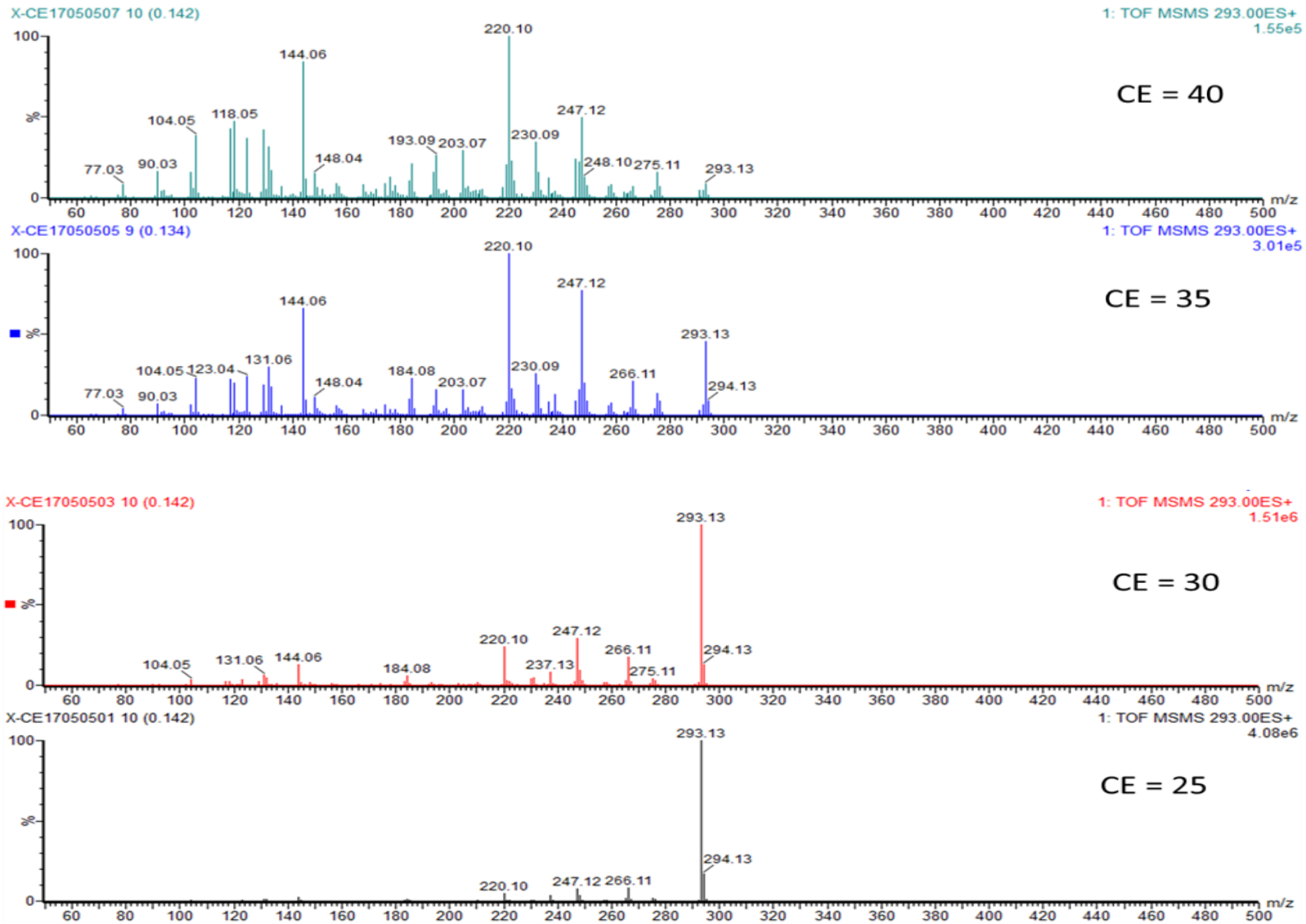
X-CE17050507 10 (0.142)
1: TOF MSMS 293.00ES+
1.55e5
CE = 40
X-CE17050505 9 (0.134)
1: TOF MSMS 293.00ES+
3.01e5
CE = 35
X-CE17050503 10 (0.142)
1: TOF MSMS 293.00ES+
1.51e6
CE = 30
X-CE17050501 10 (0.142)
1: TOF MSMS 293.00ES+
4.08e6
CE = 25
m/z
%

Supplemental Fig. 2. Representative MRM chromatograms of (A) blank rat plasma; (B) blank rat plasma spiked with EAPB02303 and EAPB02302 at the LLOQ and internal standard (EAPB0602) at 125 ng/mL; (C) blank rat plasma spiked EAPB02303 and EAPB02302 at 1000 ng/mL and internal standard (EAPB0602) at 125 ng/mL.

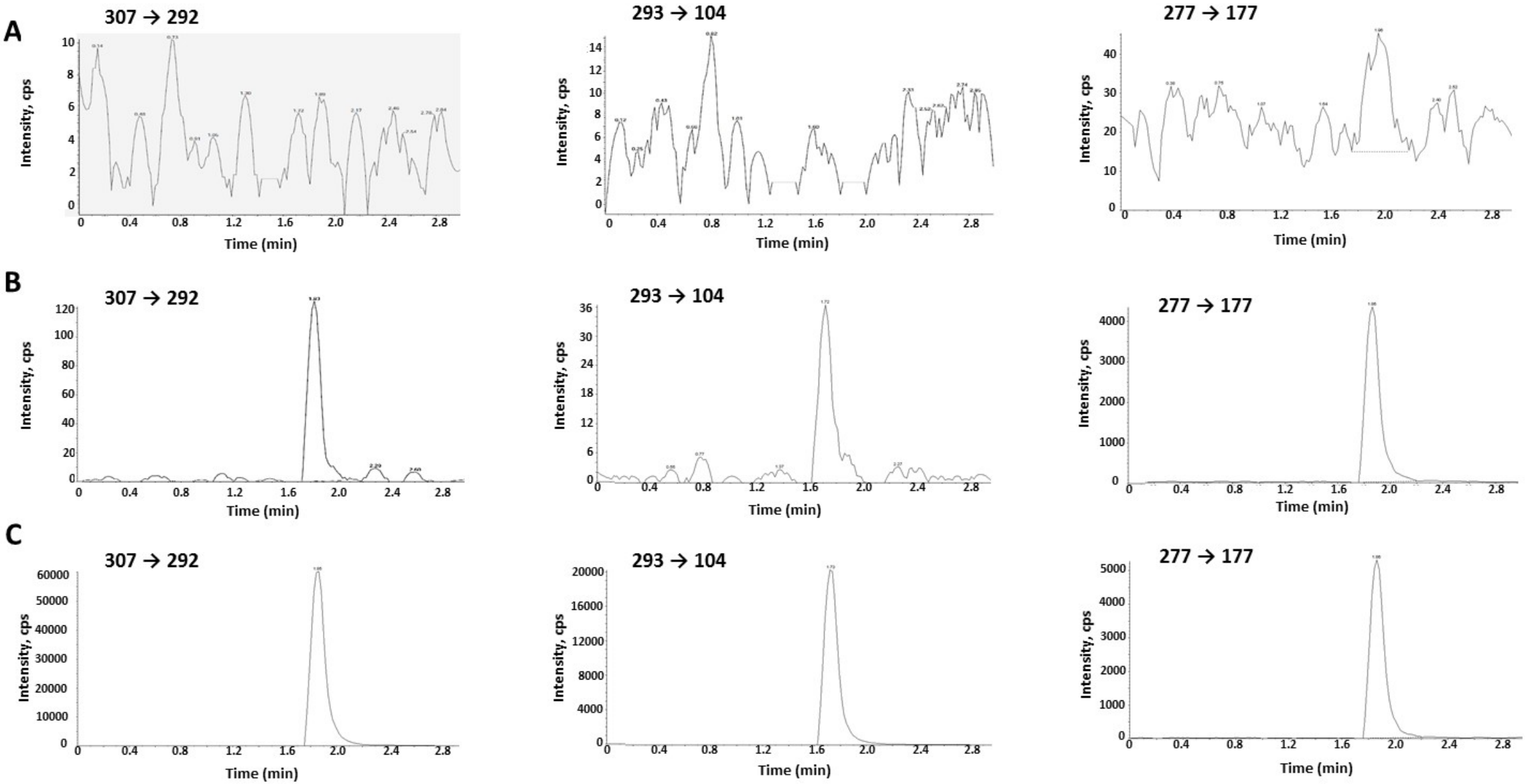

Supplemental Fig. 3. Residuals versus theoretical concentrations for EAPB02303 (A) and EAPB02302 (B) calculated concentrations, from calibration curves performed in rat plasma.